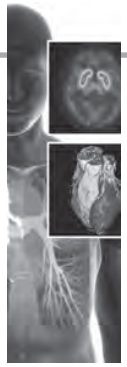

Breast-specific gamma imaging in a breast cancer center: adjunct to characterization of suspicious lesions and supporting therapeutic decisions

Perception and characterization of breast lesions are decisive for radiologists. Structural breast changes are assessed with morphologic imaging modalities, which are also used to guide biopsies of breast lesions. However, the biologic behavior of a breast lesion cannot be estimated reliably with these techniques - and if at all, then only indirectly, for example by evaluation of the margin characteristics. By prospectively introducing Breast-specific gamma imaging (BSGI) in the work-up of suspicious breast lesions, we gained information about metabolic alterations in breast lesions, which were initially detected with conventional modalities. Due to positive correlation between the degree of radiotracer uptake of a breast lesion and its aggressiveness, the diagnostic and therapeutic approach can be influenced.

KEYWORDS: Breast-specific gamma imaging; relative uptake factor; breast cancer; tissue characterization

Thomas Meissnitzer* & Matthias Wolfgang Meissnitzer

Department of Radiology, Paracelsus Medical University Salzburg, Müllner Hauptstrasse 48, Salzburg, Salzburg 5020, Austria

**Author for correspondence:*

Tel.: +43 662 4482 58987

thomas.meissnitzer@gmail.com

Introduction

In this review we describe the role of Breast-specific gamma imaging (BSGI) compared to the established methods of breast imaging in the work-up of suspicious breast lesions. Based on our previous publications the benefits, but also the limitations of this imaging modality are outlined.

Materials and methods

Within a 15-month period (from January 2013 to March 2014) 67 females with 92 newly diagnosed breast lesions of the categories IV and V according to the breast imaging reporting and data system (BI-RADS©) were included in our initial prospective study [1,2]. After clinical examination, evaluation of mammograms (mainly performed in external institutions) and ultrasound examination, BSGI was performed at presentation according to the guidelines of the EANM using a dedicated gamma camera for BSGI Dilon 6800 [3]. 3-T breast MRI was performed within 10 days prior to image-guided biopsy. Following a strict reading order, each lesion was categorized according to BI-RADS© and final rating corresponded to the maximum BI-RADS category. Biopsy results were the reference standard. Further details concerning all imaging modalities, biopsy techniques and statistical methods applied were described in a previous publication by our group [1].

Subsequently, the 99mTechnetium SestaMIBI (99mTc SestaMIBI)-uptake of the invasive ductal cancers (IDCs) - as the numerically largest group among the detected malignant lesions - was investigated retrospectively and related to their histopathological and immunohistochemical features. The semiquantitative uptake factor implemented in our initial study was correlated to the established immunohistochemical characteristics and the subtypes of the invasive ductal cancers. Further details to this retrospective work-up, especially all histopathological and immunohistochemical analyses, as well as their interpretation were described in our study [4].

Results

Our first study highlighted the outstanding diagnostic potential of BSGI due to the highest positive predictive value for malignancy, the highest accuracy and the largest area under the curve (AUC) compared to all morphologic imaging modalities. Only the results of MRI were comparable to BSGI, as shown in **TABLE 1**. **FIGURE 1** demonstrates the ability of BSGI to characterize breast lesions, as the unsuspicious breast parenchyma with fibrosis correctly showed no SestaMIBI-uptake in contrast to the invasive ductal carcinoma behind the nipple. Both lesions were highly suspicious in mammography (MG) and ultrasound (US).

However, BSGI had two limitations: Firstly, eccentric location of a breast lesion out of the field-of-view of the BSGI camera may prevent its detection, also shown by Spanu *et al.* [5]. Secondly, we observed a drop in sensitivity of BSGI for lesions with a diameter of less than 1 cm with an average of 60%. In **FIGURE 2** an IDC occult in BSGI and mammography due to eccentric location is shown, in **FIGURE 3** a small left-sided carcinoma, also occult in BSGI is demonstrated.

Table 1. Diagnostic performance of imaging modalities (N=92).

Performance	Mammography	Breast ultrasound	Magnetic resonance imaging	Breast-specific gamma imaging
Sensitivity/TPR*	0.85 ± 0.07 (57/67)	0.99 ± 0.02 (66/67)	0.88 ± 0.07 (59/67)	0.90 ± 0.06 (60/67)
Specificity/TNR*	0.28 ± 0.09 (7/25)	0.20 ± 0.08 (5/25)	0.40 ± 0.10 (10/25)	0.56 ± 0.10 (14/25)
Precision/PPV*	0.76 ± 0.09 (57/75)	0.77 ± 0.09 (66/86)	0.80 ± 0.08 (59/74)	0.85 ± 0.07 (60/71)
NPV*	0.41 ± 0.10 (7/17)	0.83 ± 0.08 (5/ 6)	0.56 ± 0.10 (10/18)	0.67 ± 0.10 (14/21)
Accuracy*	0.70 ± 0.09 (64/92)	0.77 ± 0.09 (71/92)	0.75 ± 0.09 (69/92)	0.80 ± 0.08 (74/92)
AUC (p-value)	0.64 (0.095)	0.59 (0.041)	0.57 (0.047)	0.73
Kappa	0.15	0.24	0.31	0.48
McNemar	0.19	0.00	0.21	0.48

*Numbers for calculation in parenthesis; AUC=Area under Curve or Balanced Accuracy with p-values from DeLong's test for ROC curves compared to BSGI; McNemar=p-value for comparison of imaging modalities and histologically confirmed results. Diagnostic performance of imaging modalities, reproduced according to Meissnitzer et al. [1] with permission from The British Institute of Radiology. Results including confidence intervals are listed.

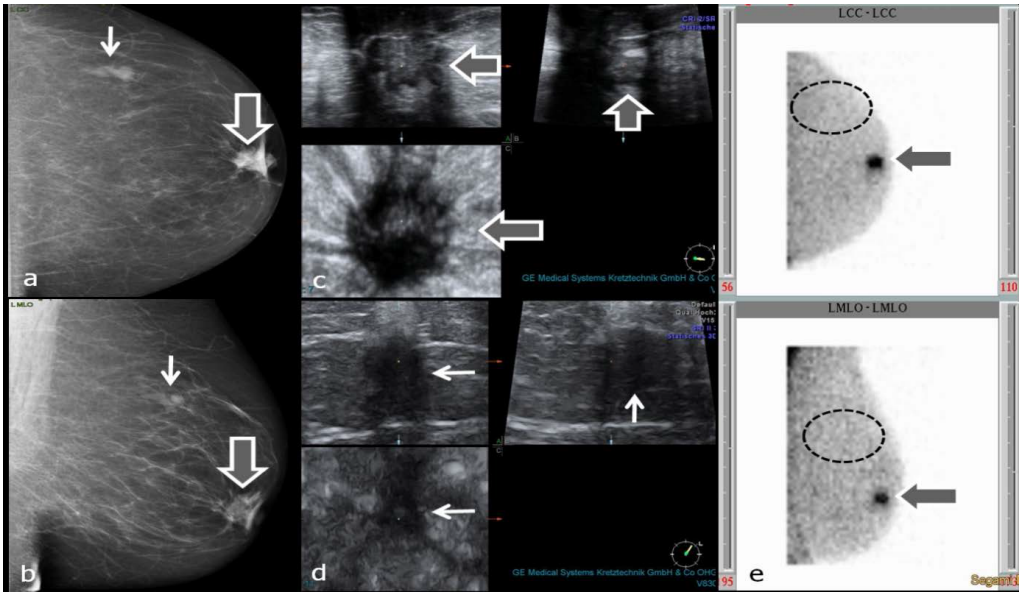

Figure 1a-1e. Characterization of mass lesions with BSGI. Reproduced according to Meissnitzer *et al.* [1] with permission from The British Institute of Radiology. Thick arrows in a-c and e point to the invasive-ductal carcinoma behind the left nipple, thin arrows in a-d point to the circumscribed breast parenchyma with fibrosis. Dashed ellipses in e encircle the region of upper-outer quadrant without tracer-uptake (assumed position of the breast parenchyma with fibrosis). a,b: MGs in craniocaudal (a) and mediolateral-oblique (b) projection; c: 3D-US of carcinoma behind the nipple; d: 3D-US of breast-parenchyma with fibrosis; e: planar BSGI in cc- (figure above) and mlo- (figure below) projection.

Among the IDCs our data showed no statistically valid correlation between the semi-quantitiative uptake factor (RUF) and the estrogen- as well as the progesterone receptor-status. Nevertheless, a reliable relationship to the KI-67 level and so to the IDC–subtypes could be demonstrated, as shown in **TABLE 2**. In particular, the distinction between luminal-A and the other subtypes of IDC could be outlined, see also **FIGURE 4**.

Discussion

We implemented BSGI as an adjunct to morphologic imaging modalities in the work-up of suspicious breast lesions in our breast cancer center of a university hospital. In this setting additional characterization of the biologic behavior of a breast lesion facilitates the decision for or against biopsy or the selection of the lesion subjected to biopsy in cases of more than one lesion.

In contrast to the screening situation these indications justify the significantly higher radiation dose of BSGI compared to mammography [6], because additional information obtainable from BSGI, such

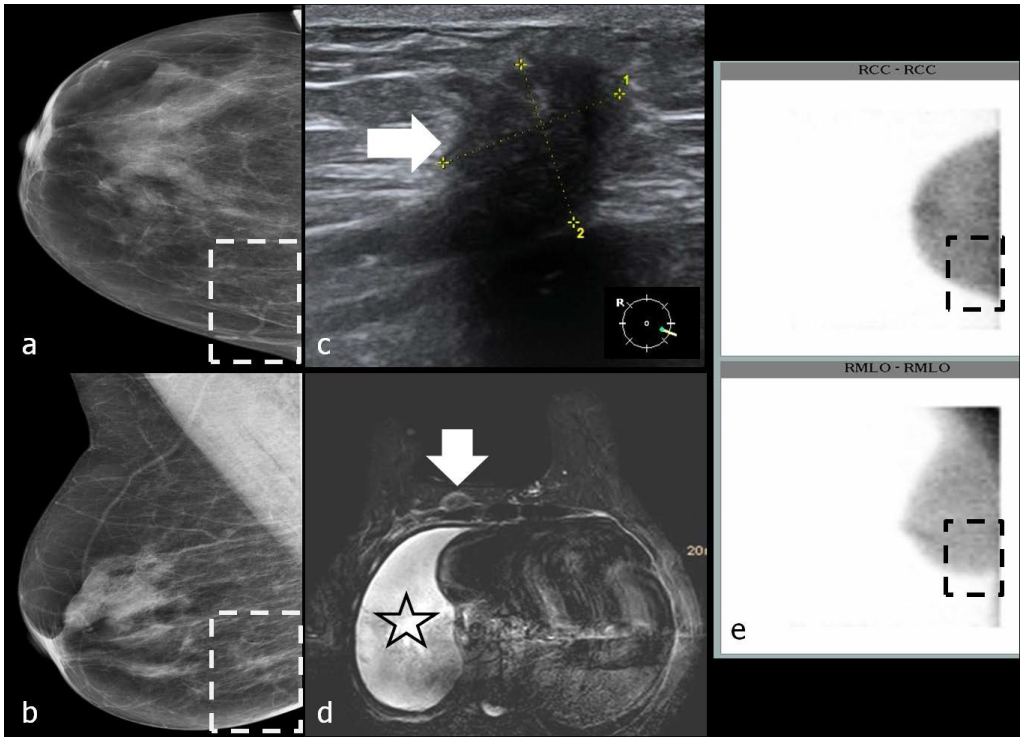

Figure 2a-2e. Occult breast carcinoma in BSGI and mammography due to eccentric location. Reproduced according to Meissnitzer *et al.* [1] with permission from The British Institute of Radiology. Thick arrows in c and d point to breast carcinoma at the right parasternal chest wall that was only detected with US and MRI due to its eccentric location. Asterisk in d marks the malignant hemorrhagic pleural effusion. Dashed rectangles in a, b and e highlight the inner lower quadrant of right breast with no hotspot detectable. a, b: MGs craniocaudal (a) and mediolateral-oblique (b) projections; c: US of the right-sided cancer; d: MRI T1w FS + Dotarem®; e: BSGIs in cc- (figure above) and mlo- (figure below)- projection.

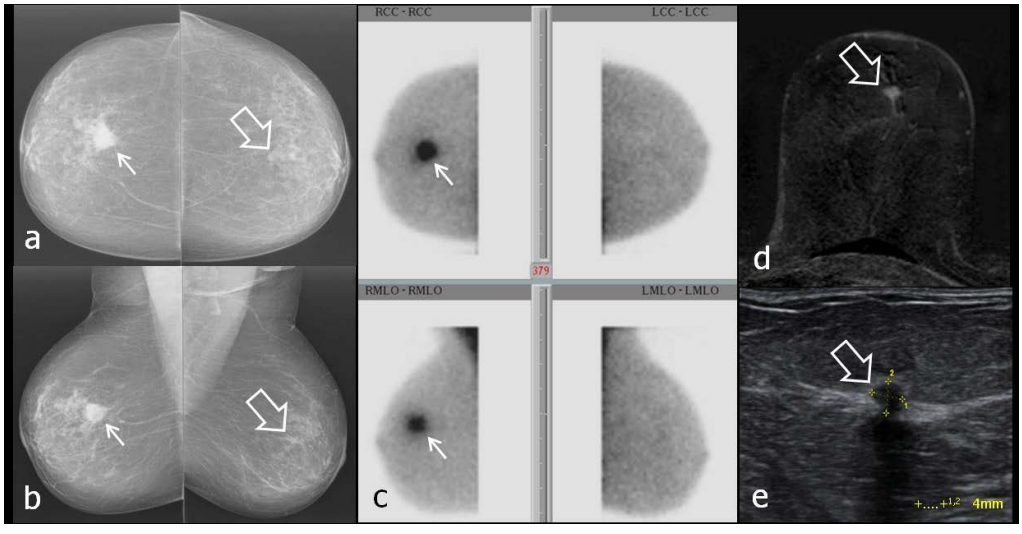

Figure 3a-3e. BSGI-occult, small left-sided carcinoma (G2). Reproduced according to Meissnitzer *et al*. [1] with permission from The British Institute of Radiology. Left breast was assessed in BSGI as category 2 according to Brem *et al.* [12]. Larger right-sided carcinoma (18 mm) was clearly seen as focal hot spot on scintigram. Thick arrows in a, b, d and e point to 4 mm left-sided carcinoma. Thin arrows in a, b and c mark the 18 mm right-sided carcinoma. a, b: Bilateral MGs craniocaudal (above) and mediolateral-oblique (below) projections; c: BSGIs of both breasts in cc (figure above) and mlo (figure below) projections; d: MRI of the left breast, T1w FS + Dotarem®; e: US of the left-sided cancer.

Table 2. Statistics of the different relative uptake factor (RUF) categories.

	RUF	Sensitivity (SE)	Specificity	(SE)	PPV	(SE)	NPV	(SE)	AUC	p-Value	Kappa	McNemar
Non-luminal-A	>2.6	0.840 (0.052)	0.520	(0.071)	0.636	(0.068)	0.765	(0.060)	0.680	(0.008)	0.360	0.080
	>3.04	0.640 (0.068)	0.600	(0.069)	0.615	(0.069)	0.625	(0.068)	0.620	(0.059)	0.240	1.000
	>6.5	0.320 (0.066)	1.000	(0.000)	1.000	(0.000)	0.595	(0.069)	0.660	(0.016)	0.320	0.000
Ki-67 >14%	>2.6	0.818 (0.055)	0.464	(0.071)	0.545	(0.070)	0.765	(0.060)	0.620	(0.239)	0.268	0.022
	>3.04	0.591 (0.070)	0.536	(0.070)	0.500	(0.071)	0.625	(0.068)	0.560	(0.559)	0.124	0.522
	>6.5	0.318 (0.066)	0.964	(0.026)	0.875	(0.047)	0.643	(0.068)	0.680	(0.057)	0.303	0.001

SE: Standard Error; PPV: Positive Predictive Value; NPV: Negative Predictive Value; AUC: Area Under the Curve. Reproduced according to Meissnitzer *et al.* [4] with permission from the International Institute of Anticancer Research.

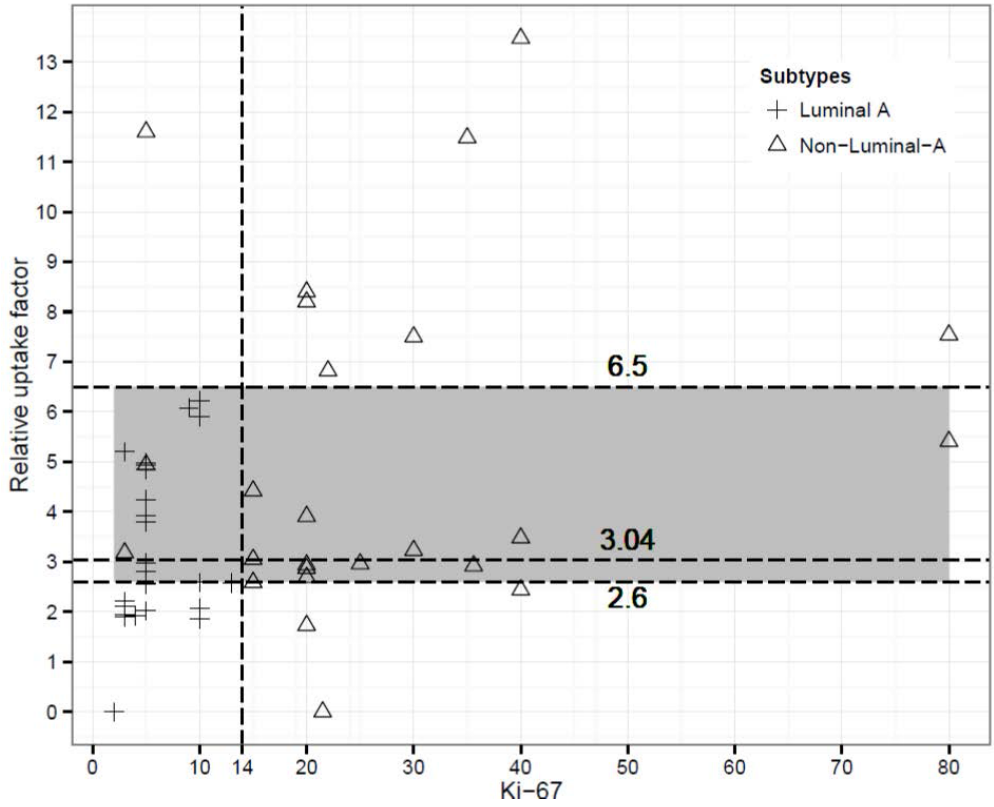

Figure 4. Correlations of the relative uptake factor (RUF), Ki-67 values and invasive ductal cancer (IDC) subtypes in the scatterplot. Reproduced according to Meissnitzer *et al*. [4] with permission from the International Institute of Anticancer Research. A relative uptake factor (RUF) of 2.6 and 6.5 can be regarded as valid thresholds.

as potential multifocality, multicentricity, bilaterality and aggressiveness of breast lesions are crucial for therapy and prognosis and may be occult in the morphologic imaging modalities [7]. The immediate benefit of these informations exceeds the possible risk of radiation-induced cancer by far.

SestaMIBI-uptake reflects the level of tissue metabolism. As a lipophilic cationic compound 99mTc SestaMIBI diffuses unspecifically from the blood into the cytoplasma and the mitochondria, depending on angiogenesis, regional perfusion and mitochondrial membrane potentials [8-10]. Our method to calculate the SestaMIBI-uptake semi-quantitatively can be used easily in daily practice and increases the validity of BSGI, although we obtained only an approximate relative uptake factor, because the size of the lesion, its distance from the detector and the breast thickness were not taken into account [11].

In our opinion, BSGI should always be analyzed in concordance with the findings of the other imaging modalities. Ultimately, BSGI negativity (scores 1 and 2 according to Brem *et al.*) may support the decision not to biopsy a lesion

with low or moderate prevalence for malignancy of up to 10% (BI-RADS III or IVa lesions) in the morphologic imaging modalities [12].

Quantification of the lesions uptake can be of particular importance for the characterization of IDCs. IDCs are a heterogeneous entity concerning prognosis and therapy [13]. Although hormone receptor status and proliferation markers are examined in biopsy specimen, BSGI may improve the reliability of diagnosis, because histopathological and immunohistochemical analyses of biopsy specimen are limited due to small sample volume, heterogeneous expression, different lab methods and subjective reading [14]. If an IDC exceeds a diameter of 1 cm, these limitations are irrelevant for BSGI. Moreover, sample error may be obviated, because radiologists can select the area with the highest tracer uptake within a lesion for their biopsy, pointing to the most dedifferentiated and thus most aggressive part.

In our study a RUF higher than 6.5 indicated a highly aggressive nonluminal-A IDC subtype, whereas a RUF below 2.6 pointed to a less aggressive luminal-A subtype. In former studies, e.g., by Voduc *et al.*, luminal-A IDCs exhibited a much lower local recurrence rate of 8% within 10 years compared to nonluminal A-IDCs (Her2/Neu-positive and triple negative) of 21% and 13%, respectively [15]. Patients with nonluminal-A carcinomas and higher Ki-67 levels typically suffer from liver and brain metastasis and expect a shorter disease-free interval compared to patients with luminal-A IDCs, who may preferably develop bone metastasis [16-18]. However, nonluminal and thus dedifferentiated IDC-subtypes show a better response to chemotherapy with the highest rates for triple-negative and Her2/Neu-enriched IDCs, a fact known as the ´triple-negative paradox´ [19]. On the other hand, patients with luminal-A IDCs would expect little benefit from chemotherapy, even though they would be exposed to the side-effects [20].

Conclusion

BSGI with the easily calculated semi-quantitative uptake factor is a valuable tool in an assessment center, not only for characterization and classification of breast lesions, but also for the assessment of their prognosis and making therapy decisions.

REFERENCES

1. Mitchell ME, Rushton FW Jr, Boland AB *et al.* Emergency procedures on the descending thoracic aorta in the endovascular era. *J. Vasc. Surg.* 54, 1298-1302 (2011).
2. Demetriades D, Velmahos GC, Scalea TM *et al.* Operative repair or endovascular stent graft in blunt traumatic thoracic aortic injuries: results of an American Association for the Surgery of Trauma Multicenter Study. *J. Trauma.* 64, 561-570 (2008).
3. Cowley RA, Turney SZ, Hankins JR *et al.* Rupture of thoracic aorta caused by blunt trauma. A fifteen-year experience. *J. Thorac. Cardiovasc. Surg.* 100, 652-660 (1990).
4. Ott MC, Stewart TC, Lawlor DK *et al.* Management of blunt thoracic aortic injuries: endovascular stents versus open repair. *J. Trauma.* 56, 565-570 (2004).
5. Fabian TC, Richardson JD, Croce MA *et al.* Prospective study of blunt aortic injury: multicenter trial of the American Association for the Surgery of Trauma. *J. Trauma.* 42, 374-380 (1997).
6. Martinelli O, Malaj A, Gossetti B *et al.* Outcomes in the emergency endovascular repair of blunt thoracic aortic injuries. *J. Vasc. Surg.* 58, 832-835 (2013).
7. Marone EM, Kahlberg A, Tshomba Y *et al.* Single-center experience with endovascular treatment of acute blunt thoracic aortic injuries. *J. Cardiovasc. Surg. (Torino).* 54, 123-131 (2013).
8. Echeverria AB, Branco BC, Goshima KR *et al.* Outcomes of endovascular management of acute thoracic aortic emergencies in an academic level 1 trauma center. *Am. J. Surg.* 208, 974-980 (2014).
9. Farber MA, Giglia JS, Starnes BW *et al.* TAG 08-02 clinical trial investigators, Evaluation of the redesigned conformable GORE TAG thoracic endoprosthesis for traumatic aortic transection. *J. Vasc. Surg.* 58, 651-658 (2013).
10. Khoynezhad A, Azizzadeh A, Donayre CE *et al.* RESCUE investigators. Results of a multicenter, prospective trial of thoracic endovascular aortic repair for blunt thoracic aortic injury (RESCUE trial). *J. Vasc. Surg.* 57, 899-905 (2013).
11. Lee WA, Matsumura JS, Mitchell RS *et al.* Endovascular repair of traumatic thoracic aortic injury: clinical practice guidelines of the Society for Vascular Surgery. *J. Vasc. Surg.* 53, 187-192 (2011).
12. Kilic A, MD, Shah AS *et al.* Trends in repair of intact and ruptured descending thoracic aortic aneurysms in the United States: a population-based analysis. *J. Thorac. Cardiovasc. Surg.* 147, 1855-1860 (2014).
13. Schermerhorn ML, Giles KA, Hamdan AD *et al.* Population-based outcomes of open descending thoracic aortic aneurysm repair. *J. Vasc. Surg.* 48, 821–827 (2008).
14. Barbato JE, Kim JY, Zenati M *et al.* Contemporary results of open repair of ruptured descending thoracic and thoracoabdominal aortic aneurysms. *J. Vasc. Surg.* 45, 667–676 (2007).
15. Girardi LN, Krieger KH, Altorki NK *et al.* Ruptured descending and thoracoabdominal aortic aneurysms. *Ann. Thorac. Surg.* 74, 1066-1070 (2002).
16. Gopaldas RR, Dao TK, LeMaire SA *et al.* Endovascular versus open repair of ruptured descending thoracic aortic aneurysms: a nationwide risk-adjusted study of 923 patients. *J. Thorac. Cardiovasc. Surg.* 142, 1010-1018 (2011).
17. Jonker FH, Verhagen HJ, Lin PH *et al.* Outcomes of endovascular repair of ruptured descending thoracic aortic aneurysms. *Circulation.* 121, 2718-2723 (2010).
18. Minami T, Imoto K, Uchida K *et al.* Clinical outcomes of emergency surgery for acute type B aortic dissection with rupture. *Eur. J. Cardiothorac. Surg.* 44: 360-364 (2013).
19. Trimarchi S, Nienaber CA, Rampoldi V *et al.* IRAD Investigators .Role and results of surgery in acute type B aortic dissection: insights from the International Registry of Acute Aortic Dissection (IRAD). *Circulation.* 114, 1357-1364 (2006).
20. Shu C, Fang K, Luo M *et al.* Emergency endovascular stent-grafting for acute type B aortic dissection with symptomatic

malperfusion. *Int. Angiol.* 32, 483-491 (2013).

21. Heneghan RE, Singh N, Starnes BW. Successful emergent endovascular repair of a ruptured mycotic thoracic aortic aneurysm. *Ann. Vasc. Surg.* 29, 843 (2015).
22. Canaud L, D'Annoville T, Ozdemir BA *et al.* Combined endovascular and surgical approach for aortobronchial fistula. *J. Thorac. Cardiovasc. Surg.* 148, 2108-2111 (2014).